Sliding Window-Frequency Domain Equalization for Multi-mode Communication Systems

Jialing Li[1], Erdem Bala[2], Rui Yang[3]
InterDigital Communications Inc.
Melville, NY
Jialing.Li@interdigital.com[1], Erdem.Bala@interdigital.com[2], Rui.Yang@interdigital.com[3]

Abstract— **Future wireless communications should be designed efficiently to support multi-mode operations for different types of applications, such as machine-to-machine, video streaming, web browsing and voice. In the physical layer multi-mode operation could include the coexistence of single carrier and multicarrier modulations. To reduce overall complexity and power consumption, it is highly desirable to design the receiver such that some of the components are shared or reused by multiple modulation schemes. In this paper we propose a receiver architecture which is composed of a common channel equalizer for all carrier modulation schemes. Furthermore, we investigate the feasibility of using a well-studied time domain equalizer designed for single carrier modulation, i.e., the sliding window-frequency domain equalizer (SW-FDE) for general multicarrier modulation (MCM) receivers. As a specific illustration of the concept, we present the application of this equalizer to an OFDM-offset QAM system.**

Keywords-multi-mode system; orthogonal frequency division multiplexing-offset quadrature amplitude modulation; OFDM-OQAM; equalization

I. INTRODUCTION

MCM techniques enable transmission of a set of data over multiple narrow band subcarriers simultaneously. With an advanced wideband modulation and coding scheme, a system with MCM can achieve much higher spectral efficiency in frequency selective channels compared to those using single carrier modulation techniques. Orthogonal Frequency Division Multiplexing (OFDM) may be the most well-known MCM scheme that has been used in many standardized systems [1]. To support future systems with high spectral agility, such as cognitive radio, Filter Bank Multicarrier, e.g., OFDM-offset QAM (OFDM-OQAM), and its application to various multiple access systems have been investigated by many researchers recently [2].

OFDM can be considered as a type of filter bank multicarrier (FBMC) modulation whose time domain prototype filter is a simple rectangular pulse. Such a pulse, however, introduces large sidelobes, which create several challenging issues in practical systems, including high sensitivity to frequency offsets and large out-of-band emissions (OOBE). In OFDM-OQAM, a carefully designed prototype filter is used so that OOBE is much less than that of OFDM [3], [4]. The signals of adjacent subcarriers overlap each other to achieve a high spectral efficiency. Different from OFDM, the real and imaginary parts of the QAM symbols are processed separately with 2×symbol rate. A prototype filter needs to be carefully designed to minimize or zero out ISI and ICI while keeping the side lobes small.

In general, the channel equalization for OFDM-OQAM in fading channels could be grouped into two main categories: The first one is equalization before the OFDM-OQAM analysis filter bank (AFB), which may require using a cyclic prefix (CP) in the transmit signal and results in low spectral efficiency and large OOBE [2], [5]. The second one is equalization after the OFDM-OQAM AFB, e.g., the most popular subcarrier-based equalization, with single tap or multiple taps [6]-[18]. It has been shown that even in mildly selective channels, a per-subcarrier multi-tap equalizer is needed for decent BER performance. Therefore, it is evident that to achieve good performance in highly frequency selective channels with long delay spreads, a very complex equalizer is required.

In this paper, we consider using the sliding window frequency domain equalizer (SW-FDE) [19] in multi-mode systems. The equalizer is applied to the received signals before demodulation, and therefore, can be applied to MCM as well as single-carrier (SC) signals. As a specific illustration of the concept, we present the application of this equalizer to an OFDM-OQAM system, where the equalization is performed before the AFB. The same idea has been used in single carrier systems [19]-[20] as well as OFDM systems [21].

The proposed equalizer uses a sliding window to perform equalization for the central portion of the samples of each window (block) and slides the window along the block to cover all received samples. In the equalization of each block, it approximates the system model as if the channel impairment is a circular convolution with the channel impulse response. The inherent interference due to this approximation is analyzed. Simulations show that the SW-FDE outperforms the simple and practical single-tap minimum mean square error (MMSE) equalizer after the OFDM-OQAM AFB in terms of raw BER performance in highly selective channels. The raw BER performance due to inherent interference is also compared for different block lengths.

The rest of the paper is organized as follows: In Sec. II, the OFDM-OQAM system model and architecture is presented. Our proposed SW-FDE is described in Sec. III. Then, simulation results for practical channel models are given in Sec. IV, followed by conclusions in Sec. V.

978-1-4577-1343-9/12/$26.00 ©2013 IEEE

II. System Model and Architecture

Without loss of generality, in this paper, we consider a FBMC system based on OFDM-OQAM shown in Figure 1, in which the SW-FDE along with a channel estimator is set before the AFB. The detailed description of the SW-FDE will be given in the next section.

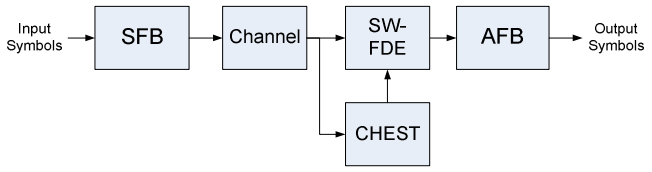

Figure 1. The high level system architecture

The synthesis filter bank (SFB) and AFB of the system based on OFDM-OQAM may be implemented in several ways; each has different complexity in terms of number of arithmetic calculations. The structures of the SFB and AFB in this paper are shown in Figure 2. This design requires that the prototype filter length, L_p, is an odd number.

In Figure 2, L is the FFT size, $M(\leq L)$ is the number of active subcarriers, and $b = \frac{L_p-1}{2}$. $\{s_k^O[n], k = 0, \dots, M-1\}$ are the OQAM modulated, real valued, symbols. And, $\{A_k(z), k = 0, \dots, L-1\}$ is the polyphase filters (with respect to L) of the corresponding prototype filter, in which $A_k(z) = \sum_{m=0}^{\lceil L_p/L \rceil - 1} p_e[q+mL]z^{-m}$ and $p_e[n]$ is the prototype filter coefficients. The permutation operation in Figure 2(a), $\boldsymbol{P}_{\pi b}$, for an integer b is defined by the permutation matrix

$$\mathbf{P}_{\pi b} = \begin{bmatrix} \mathbf{0}_{b\times(L-b)} & \mathbf{I}_b \\ \mathbf{I}_{L-b} & \mathbf{0}_{(L-b)\times b} \end{bmatrix} \quad (1)$$

where $\mathbf{I}_x$ is the rank-x identity matrix and $\mathbf{0}_{x\times y}$ is an x by y zero matrix. And the permutation operation in Figure 2(b), is defined by the permutation matrix

$$\mathbf{P}_{\pi a} = \begin{bmatrix} 1 & 0 & \cdots & \cdots & 0 \\ 0 & \cdots & \cdots & 0 & 1 \\ 0 & \cdots & 0 & 1 & 0 \\ \vdots & \iddots & \iddots & \iddots & \vdots \\ 0 & 1 & 0 & \cdots & 0 \end{bmatrix} \mathbf{P}_{\pi b}^T \quad (2)$$

It should be mentioned that the AFB can be implemented using either an FFT or an IFFT. Here, similar to [4], we choose to use the FFT based implementation of AFB since it can fall back to OFDM operation to enable a multi mode design, even though the IFFT based implementation could be less complex. On the other hand, comparing to the design in [4], the proposed SFB and AFB with permutation operation can provide a less complex implementation.

Regarding the structure shown in Figure 1, channel estimation is performed before the AFB. In practice, this can be achieved by attaching a preamble with reference signals for each block of transmitted OFDM-OQAM modulated signals, similar to 802.11 standards [22]. As an alternative, channel may be estimated after the AFB by using scattered pilots [23]. However, this would result in a delay and higher complexity since the received signal has to be processed by the AFB twice.

The use of a channel equalizer prior to the demodulation process does not depend on the type of waveform as long as the reference signal is designed properly to support the channel estimation. This means that the architecture shown in Figure 1 can be applied to any waveform. For a multi-mode system that supports multiple waveforms, this type of equalizer can be shared or reused so that the overall complexity and cost is reduced.

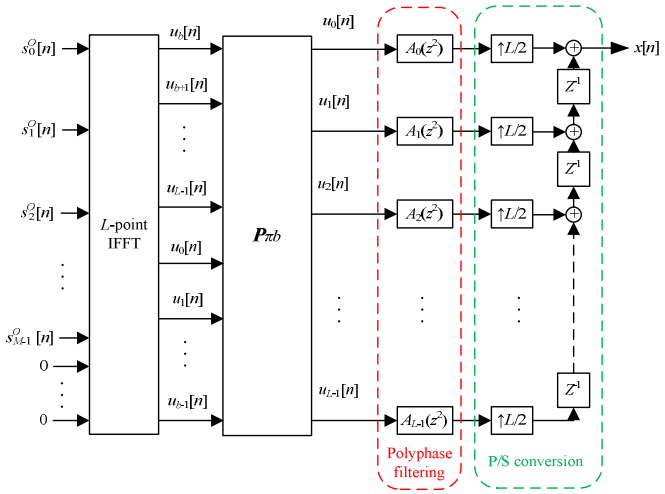

(a) Synthesis Filter Band (SFB)

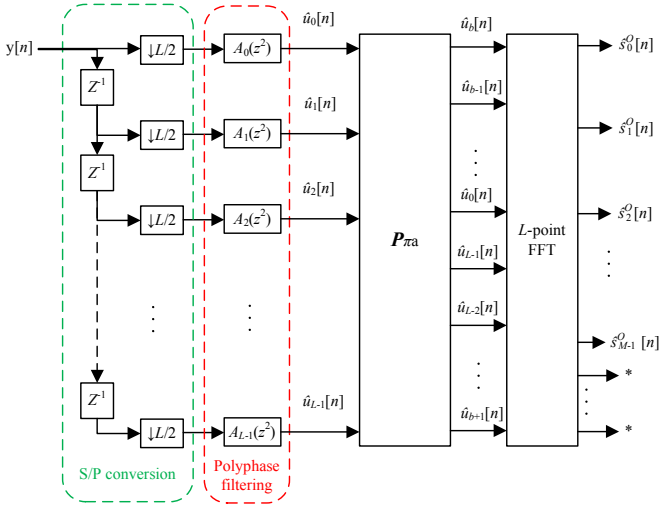

(b) Analysis Filter Bank (AFB)

Figure 2. The SFB (a) and AFB (b) of OFDM-OQAM considered in this paper

III. Sliding Window-Frequency Domain Equalizer (SW-FDE)

In this section, we introduce our proposed sliding window-frequency domain equalizer (SW-FDE) for OFDM-OQAM. It does not use a CP and hence does not introduce spectral distortion to the transmit waveform. It uses a sliding window to perform equalization for the central portion of the samples of

This work was supported by InterDigital Communications Inc.

each window (block). In the equalization of each block, it approximates the system model as if the received signal block is a circular convolution of the transmit signal block and the channel impulse response. In such an approximation, the system still suffers from inter-block interference even in the absence of noise, especially at the edges of each equalized block. Therefore, only the central portion of the equalized block is passed to the next stage of the receiver so as to minimize interference, and a sliding window is used to slide the observing window to cover all received samples.

A. SW-FDE

Sliding Window:

Assume the block length is L_b samples, and the sliding window step size is L_{ss}, which satisfies $1 \le L_{ss} \le L_b$. The total number of blocks is n_B. Denote the i^{th} length-L_b block of the SFB output $\mathbf{x}_i$ as

$$\mathbf{x}_i = [x[(i-1)L_{ss}] \quad x[(i-1)L_{ss}+1] \quad \cdots \quad x[(i-1)L_{ss}+L_b-1]]^T, i = 0,1,\cdots,n_B-1. \tag{3}$$

Note that for the 0^{th} block, the elements of x with negative indices are background interference and noise only. Due to the definition of the sliding window, if $L_{ss} < L_b$, there is overlapping between adjacent windows (blocks). As in Figure 1, there is no CP insertion. The i^{th} length-L_b block of the transmitted signal is equal to the i^{th} length-L_b block of the SFB output, i.e.,

$$\bar{\mathbf{x}}_i = \mathbf{x}_i, i = 0,1,\cdots,n_B \tag{4}$$

Also denote the i^{th} length-L_b interference block as

$$\mathbf{i}_i = [x[(i-1)L_{ss}-L_b] \quad x[(i-1)L_{ss}-L_b+1] \quad \cdots \quad x[(i-1)L_{ss}-1]]^T, i = 0,1,\cdots,n_B-1. \tag{5}$$

It has inter-block interference (IBI) to $\bar{\mathbf{x}}_i$. The sliding window operation is illustrated in Figure 3.

Channel:

Then, the i^{th} length-L_b block of the received signal is

$$\bar{\mathbf{y}}_i = \mathbf{H}_{L_b}\bar{\mathbf{x}}_i + \mathbf{H}_{\mathrm{T},L_b}\mathbf{i}_i + \bar{\mathbf{n}}_i \tag{6}$$

where the $L_b \times L_b$ Toeplitz channel matrix

$$\mathbf{H}_{L_b} = \begin{bmatrix} h_0 & 0 & \cdots & \cdots & \cdots & 0 \\ \vdots & \ddots & \ddots & \ddots & \ddots & \vdots \\ h_{L_h-1} & \cdots & h_0 & 0 & \ddots & \vdots \\ 0 & h_{L_h-1} & \cdots & h_0 & \ddots & \vdots \\ \vdots & \ddots & \ddots & \vdots & \ddots & 0 \\ 0 & \cdots & 0 & h_{L_h-1} & \cdots & h_0 \end{bmatrix} \tag{7}$$

represents the channel seen by $\bar{\mathbf{x}}_i$. The second $L_b \times L_b$ matrix

$$\mathbf{H}_{\mathrm{T},L_b} = \begin{bmatrix} 0 & \cdots & 0 & h_{L_h-1} & \cdots & h_1 \\ \vdots & \ddots & \ddots & \ddots & \ddots & \vdots \\ \vdots & \ddots & \ddots & \ddots & 0 & h_{L_h-1} \\ \vdots & \ddots & \ddots & \ddots & \ddots & 0 \\ \vdots & \ddots & \ddots & \ddots & \ddots & \vdots \\ 0 & \cdots & \cdots & \cdots & \cdots & 0 \end{bmatrix} \tag{8}$$

represents the tail end of the channel's impulse response that generates IBI to the first $L_h - 1$ samples in the succeeding block. These two matrices have the interesting property of

$$\mathbf{H}_a + \mathbf{H}_{\mathrm{T},a} = \mathbf{H}_{\mathrm{c},a} \tag{9}$$

where $\mathbf{H}_{\mathrm{c},a}$ is an $a \times a$ circulant matrix with the first column being $\left[\mathbf{h}^T \quad \mathbf{0}_{1\times(a-L_h)}\right]^T$.

FDE:

Equation (6) could be rewritten as

$$\bar{\mathbf{y}}_i = \mathbf{H}_{\mathrm{c},L_b}\bar{\mathbf{x}}_i + \hat{\mathbf{n}}_i \tag{10}$$

where the circulant matrix $\mathbf{H}_{\mathrm{c},L_b} = \mathbf{H}_{L_b} + \mathbf{H}_{\mathrm{T},L_b}$ is defined in (9), and the interference and noise is

$$\hat{\mathbf{n}}_i = \mathbf{H}_{\mathrm{T},L_b}(\mathbf{i}_i - \bar{\mathbf{x}}_i) + \bar{\mathbf{n}}_i \tag{11}$$

Note that the first $L_h - 1$ samples suffer from the interference that comes from the last $L_h - 1$ samples in $\mathbf{i}_i$ and $\bar{\mathbf{x}}_i$. Since the circulant matrix $\mathbf{H}_{\mathrm{c},L_b}$ satisfies

$$\mathbf{H}_{\mathrm{c},L_b} = \frac{1}{L_b}\mathbf{F}_{L_b}^H \mathbf{\Lambda}_h \mathbf{F}_{L_b} \tag{12}$$

where $\mathbf{F}_{L_b}$ is the $L_b \times L_b$ DFT matrix

$$\mathbf{F}_L = \begin{bmatrix} 1 & 1 & \cdots & 1 \\ 1 & W_L & \cdots & W_L^{L-1} \\ \vdots & \vdots & \ddots & \vdots \\ 1 & W_L^{L-1} & \cdots & W_L^{(L-1)(L-1)} \end{bmatrix}, \tag{13}$$

$\mathbf{F}_{L_b}^H$ is the $L_b \times L_b$ IDFT matrix, and

$$\mathbf{\Lambda}_h = diag\{\boldsymbol{\lambda}_h\} \tag{14}$$

with

$$\boldsymbol{\lambda}_h = \left[\lambda_{h,0}, \lambda_{h,1}, \ldots, \lambda_{h,L_b-1}\right]^T = \mathbf{F}_{L_b}\mathbf{h} \tag{15}$$

then, the following equalizer, which is also a circulant matrix,

$$\mathbf{E}_{L_b} = \frac{1}{L_b}\mathbf{F}_{L_b}^H \mathbf{\Lambda}_e \mathbf{F}_{L_b} \tag{16}$$

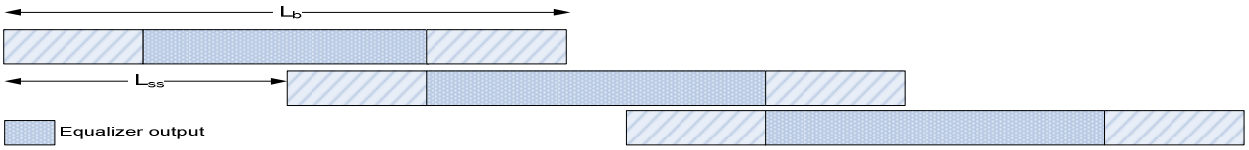

Figure 3. Sliding window operation

where

$$\mathbf{\Lambda}_e = diag\{\boldsymbol{\lambda}_e\} \tag{17}$$

with

$$\boldsymbol{\lambda}_e = \left[\lambda_{e,0}, \lambda_{e,1}, \dots, \lambda_{e,L_b-1}\right]^T \tag{18}$$

could be applied to the i^{th} block,

$$\mathbf{y}_i = \mathbf{E}_{L_b}\bar{\mathbf{y}}_i \tag{19}$$

Note that the expression of $\lambda_{e,l}$, for $l = 0, \dots, L_b - 1$, depends on the type of equalizer. In a minimum mean square error (MMSE) approach,

$$\mathbf{E}_{MMSE,L_b} = \sigma_x^2 \mathbf{H}_{\mathrm{c},L_b}^H \left(\sigma_x^2 \mathbf{H}_{\mathrm{c},L_b}\mathbf{H}_{\mathrm{c},L_b}^H + \sigma_n^2 \mathbf{I}_{L_b}\right)^{-1} \tag{20}$$

where it is assumed that $E(\mathbf{x}_i\mathbf{x}_i^H) = \sigma_x^2\mathbf{I}_{L_b}$ and $E(\hat{\mathbf{n}}_i\hat{\mathbf{n}}_i^H) = \sigma_n^2\mathbf{I}_{L_b}$. Substituting (12) into (20), after some math manipulations, we obtain

$$\mathbf{E}_{MMSE,L_b} = \frac{1}{L_b}\mathbf{F}_{L_b}^H \mathbf{\Lambda}_{e,MMSE}\mathbf{F}_{L_b} \tag{21}$$

where

$$\mathbf{\Lambda}_{e,MMSE} = \sigma_x^2 \mathbf{\Lambda}_h^H \left(\sigma_x^2 \mathbf{\Lambda}_h\mathbf{\Lambda}_h^H + \sigma_n^2\mathbf{I}_{L_b}\right)^{-1} \tag{22}$$

i.e.,

$$\lambda_{e,MMSE,q} = \frac{\lambda_{h,q}^* \sigma_x^2}{\left|\lambda_{h,q}\right|^2\sigma_x^2 + \sigma_n^2}, q = 0,1,\cdots,L_b - 1 \tag{23}$$

The MMSE equalizer in (20) could be implemented by using an L_b-point DFT, a 1-tap FDE (i.e., with the $\lambda_{e,q}$-multipliers), and an L_b-point IDFT. Note that due to the block-wise operation, the equalizer itself should have an S/P and P/S conversion pair. The P/S conversion in the equalizer could be combined with the S/P conversion in the OFDM-OQAM AFB to reduce latency.

B. *Inherent Interference Analysis*

After the FDE, all recovered samples suffer from interference from the last $L_h - 1$ samples in $\mathbf{i}_i$ and $\bar{\mathbf{x}}_i$. Substituting (10) and (11) into (19), the recovered block becomes

$$\mathbf{y}_i = \bar{\mathbf{x}}_i + \mathbf{E}_{L_b}\mathbf{H}_{\mathrm{T},L_b}(\mathbf{i}_i - \bar{\mathbf{x}}_i) + \mathbf{E}_{L_b}\bar{\mathbf{n}}_i \tag{24}$$

where $\mathbf{E}_{L_b}\mathbf{H}_{\mathrm{T},L_b}(\mathbf{i}_i - \bar{\mathbf{x}}_i)$ is the residual interference or estimation error. To analyze the residual interference, we consider the case in the absence of noise. In this case, $\mathbf{E}_{L_b}$ is essentially $\mathbf{H}_{\mathrm{c},L_b}^{-1}$, and the noise term $\mathbf{E}_{L_b}\bar{\mathbf{n}}_i$ is zero. Examples of the interference powers to each sample are shown for $L_b = L = 1024$ samples/block and $L_b = 2L = 2048$ samples/block, respectively, in Figure 4 for a 600-channel OFDM-OQAM system with 1024 samples per symbol duration. The blocks are quartered using dotted lines. As can be seen from this figure, the edge quarters have much higher interference than the middle of the blocks. This is the edge effect in SW-FDE. It is due to the much larger coefficients in the first and last few rows in $\mathbf{E}_{L_b}\mathbf{H}_{\mathrm{T},L_b}$. The interference level at either edges is not identical because the coefficients in first few rows of $\mathbf{E}_{L_b}\mathbf{H}_{\mathrm{T},L_b}$ have larger magnitudes than these in the last few rows. Comparing the interference powers for different window (block) sizes, we find that the interference powers of the middle half of blocks (i.e., samples $\frac{L_b}{4}+1, \frac{L_b}{4}, \cdots, \frac{3L_b}{4}$ of each block) become smaller as the block size increases. The suggests an appropriate sliding window step size to be $L_{ss} = \frac{L_b}{2}$.

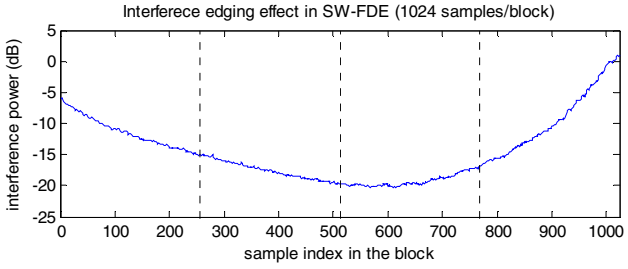

(a) SW-FDE with $L_b = L = 1024$

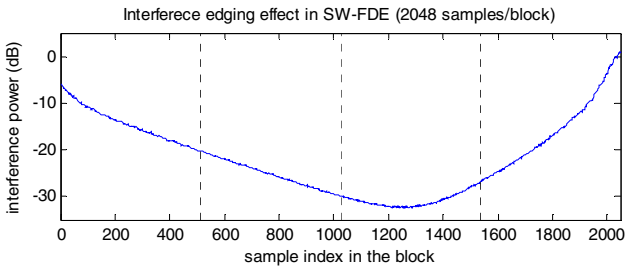

(b) SW-FDE with $L_b = 2L = 2048$

Figure 4. Interference edging effect in SW-FDE

C. *Complexity and Latency Discussion*

The complexity of the FDE is introduced by the L_b-point DFT and IDFT, and the $\lambda_{e,q}$-multipliers. The total additional number of real multiplications per block is $\mu_{SW-FDE} = 2\mu_{FFT}^C(L_b, L_b) + 4L_b = 2L_b\log_2 L_b - 2L_b + 8$. Note that the complexity of calculating the $\lambda_{e,q}$-multipliers is not included here since the $\lambda_{e,q}$-multipliers are assumed given by the channel estimation block. Assume the total number of sample of the frame is $L_t = n_B L_b$. If $L_{ss} = \frac{L_b}{2}$, its total complexity is $2n_B(2L_b\log_2 L_b - 2L_b + 8) = 4L_t\left[\log_2 L_b - 1 + \frac{4}{L_b}\right] = 4L_t\left[d - 1 + \frac{4}{2^d}\right]$, where $L_b = 2^d$. Therefore, as d, and correspondingly L_b, get larger, complexity increases.

SW-FDE uses a $1{:}\,L_b$ S/P and $L_b{:}\,1$ P/S pair and replaces the $1{:}\,L$ S/P conversion in the OFDM-OQAM AFB. Therefore, the additional inherent latency is $\tau_{SW-FDE} = L_bT_s - LT_s = T_b - T$.

IV. SIMULATIONS

In this section, we present the simulation setup and results.

A. Simulation Setup

The performance of the SW-FDE equalizer is evaluated with simulations and compared to the single-tap MMSE equalizer. Since the discussion of different equalization (e.g., multi-tap equalizers) after OFDM-OQAM AFB is not the focus of the paper, we only consider the single-tap MMSE equalizer here that is widely used in existing OFDM systems and recommended for OFDM-OQAM systems in mildly frequency selective channels. The point is to demonstrate that our proposed SW-FDE would provide satisfying BER performance for multi-mode systems, e.g., an OFDM-OQAM system, in mildly and highly selective fading channels. The simulation parameters are selected to match the widely used LTE parameters [24]. Specifically, 1024 subcarriers, of which 600 are loaded with data, are used. The subcarrier spacing is set to be 15 kHz and the block size used in the SW-FDE is chosen as $L_b = 4L = 4096$. Two vehicular channel models, Vehicular-A (Veh-A) and Vehicular-B (Veh-B), specified by the ITU-R [25] are used. The Doppler shift is set to 5 Hz for both channel models. Veh-A is a moderately selective channel with rms delay spread of 0.37μs while Veh-B is a highly selective with rms delay spread of 4μs. The parameters for the channel models are given in Table I.

TABLE I. CHANNEL MODELS USED IN THE SIMULATIONS

Tap	Vehicular A		Vehicular B	
	Delay (ns)	*Average power (dB)*	*Delay (ns)*	*Average power (dB)*
1	0	0	0	-2.5
2	310	-1	300	0
3	710	-9	8900	-12.8
4	1090	-10	12900	-10
5	1730	-15	17100	-25.2
6	2510	-20	20000	-16

B. Simulation Results in Practical Channel Models

Figure 5 illustrates the raw BER of the OFDM-OQAM system with the single-tap equalizer and SW-FDE, respectively, when the Veh-A channel model is used. We can see from this figure that the performance of the two equalizers are very close to each other with the SW-FDE showing a slightly better performance than the single-tap equalizer at high SNR.

Figure 6 illustrates the raw BER of the OFDM-OQAM system with the single-tap equalizer and SW-FDE when the Veh-B channel model is used. We can see from this figure that the SW-FDE equalizer outperforms the single-tap equalizer at medium and high SNR range for all modulation types. Because Veh-B is a highly selective channel and the delay spread is very large, the performance of the single-tap equalizer degrades significantly. The SW-FDE equalizer, on the other hand, effectively covers the channel delay spread with a sufficiently large block size. At high SNR, however, SW-FDE experiences an error floor due to IBI. The effect of the block length L_b on the BER performance of the SW-FDE equalizer is also evaluated and the result is illustrated in Figure 7. The block length is varying and equal to $kL, k = 1, 2, \ldots, 8$. Veh-B channel model is used in this simulation with infinite SNR. As we can see from the figure, the BER reduces with increasing block length. However, the rate of this reduction decreases with increasing block length. Comparing Figure 6 and Figure 7, we could see that with sufficiently large block size (i.e., $L_b \geq 3L$), SW-FDE outperforms the single-tap equalizer.

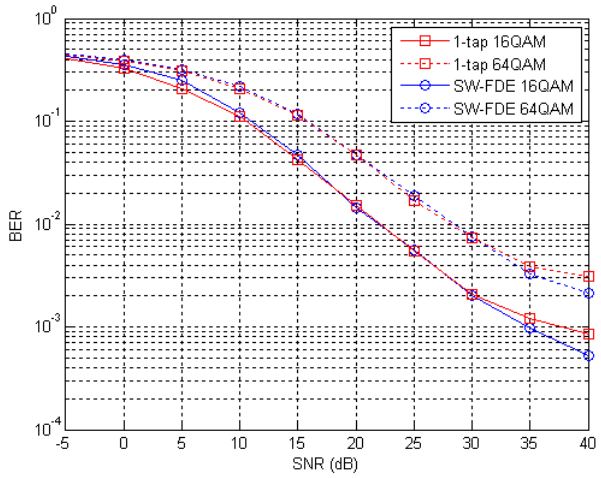

Figure 5. Raw BER performance of OFDM-OQAM in Veh-A channel

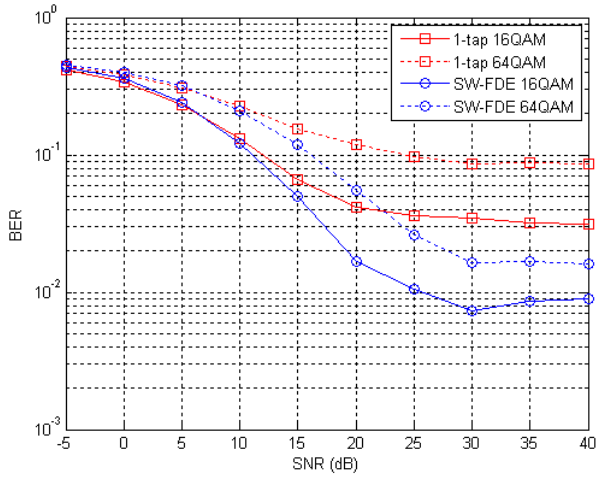

Figure 6. Raw BER performance of OFDM-OQAM in Veh-B channel

V. CONCLUSION

A sliding window frequency domain equalizer for multi-mode systems, has been introduced in this paper. As opposed to the existing equalizers that are used after the AFB, the proposed equalizer operates on the time-domain received signal, before the AFB. As such, the proposed equalizer can be used for equalization in multi-mode systems when different waveforms are supported. As a specific illustration of the concept, we present the application of this equalizer to an OFDM-OQAM system. The performance of the proposed equalizer has been evaluated in OFDM-OQAM systems with simulations and achieved better BER performance than the per subcarrier single-tap equalizer under highly selective channels with large delay spread.

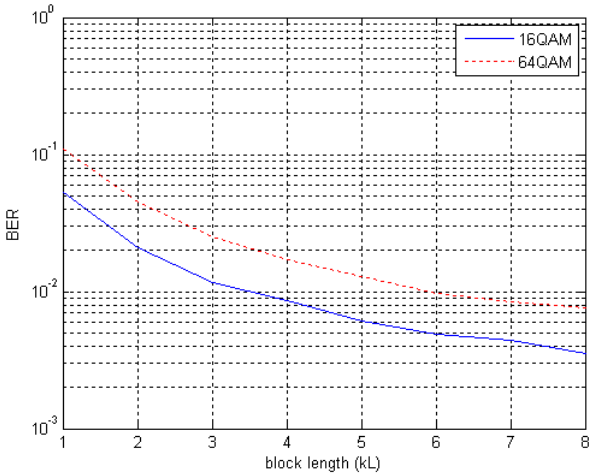

Figure 7. Raw BER performance of the SW-FDE with varying block length under the Veh-B channel

REFERENCES

[1] B. Farhang-Boroujeny, "OFDM Versus Filter Bank Multicarrier," IEEE *Signal Processing Magazine,* vol.28, no.3, pp.92-112, May 2011.

[2] A. Sahin, I. Guvenc, and H. Arslan, "A Survey on Prototype Filter Design for Filter Bank Based Multicarrier Communications," Online: http://arxiv.org/pdf/1212.3374.pdf

[3] A. Viholainen, T. Ihalainen, T. Hidalgo, M. Renfors and M. Bellanger. "Prototype filter design for filter bank based multicarrier transmission," in Proc. of 17th European Signal Processing Conference, Aug. 2009.

[4] A. Viholainen, M. Bellanger and M. Huchard, "Prototype filter and structure optimization," Physical Layer for Dynamic Spectrum Access and Cognitive Radio, Jan. 2009.

[5] H. Lin and P. Siohan, "A new transceiver system for the OFDM/OQAM modulation with cyclic prefix," in Proc. of IEEE 19th International Symposium on Personal, Indoor and Mobile Radio Communications (PIMRC), Sep. 2008.

[6] J. Louveaux, M. Tanda, M. Renfors, L. Baltar, A. Ikhlef, T. Hidalgo-Stitz, M. Bellanger, and C. Bader, "Optimization of transmitter and receiver," PHYDYAS report, Jul. 2009.

[7] A. Viholainen, J. Alhava, and M. Renfors, "Efficient implementation of complex modulated filter banks using cosine and sine modulated filter banks," EURASIP Journal on Advances in Signal Processing, vol. 2006, Article ID 58564, 10 pages, doi: 10.1155/ASP/2006/58564, 2006.

[8] J. Louveaux, L. Baltar, D. Waldhauser, M. Renfors, M. Tanda, C. Bader, and E. Kofidis, "Equalization and demodulation in receiver (single antenna)," PHYDYAS report, Jul. 2008.

[9] T. Ihalainen, A. Ikhlef, J. Louveaux, and M. Renfors, "Channel equalization for multi-antenna FBMC/OQAM receivers," IEEE Transactions on Vehicular Technology, vol. 60, no. 5, Jun. 2011.

[10] T. H. Stitz, T. Ihalainen, A. Viholainen, and M. Renfors, "Pilot-based synchronization and equalization in filter bank multicarrier communications," EURASIP Journal on Advances in Signal Processing, Vol. 2010, Article ID 741429, 18 pages, doi: 10.1155/2010/741429, 2010.

[11] G. Lin, L. Lundheim, and N. Holte, "On efficient equalization for OFDM/OQAM systems," the 10th OFDM-Workshop, Aug. 2005.

[12] D. S. Waldhauser, L. G. Baltar, and J. A. Nossek, "MMSE subcarrier equalization for filter bank based multicarrier systems," in Proceedings of IEEE Workshop on Signal Processing Advances in Wireless Communications (SPAWC'08), Jul. 2008.

[13] R. Nour, P. Pedrosa, J. Louveaux and F. Horlin, "Frequency selective channel equalization for filter bank multi-carrier modulation," the 32nd WIC Symposium on Information Theory, May 2011.

[14] D. S. Waldhauser, L. G. Baltar, and J. A. Nossek, "Adaptive equalization for filter bank based multicarrier systems," in Proceedings of IEEE International Symposium on Circuits and Systems (ISCAS'08), May 2008.

[15] A. lkhlef and J. Louveaux, "An enhanced MMSE per subchannel equalizer for highly frequency selective channels in FBMC/OQAM systems," in Proceedings of IEEE Workshop on Signal Processing Advances in Wireless Communications (SPAWC'09), Jun. 2009.

[16] L. G. Baltar, D. S. Waldhauser, and J. A. Nossek, "MMSE subchannel decision feedback equalization for filter bank based multicarrier systems," in Proceedings of IEEE International Symposium on Circuits and Systems (ISCAS'09), May 2009.

[17] D. S. Waldhauser, L. G. Baltar, and J. A. Nossek, "Adaptive decision feedback equalization for filter bank based multicarrier," in Proceedings of IEEE International Symposium on Circuits and Systems (ISCAS'09), May 2009.

[18] M. Nájar, C. Bader, F. Rubio, E. Kofidis, M. Tanda, J. Louveaux, M. Renfors, and D. L. Ruyet, "MIMO channel matrix estimation and tracking," PHYDYAS report, Jan. 2009.

[19] A. Reznik, R. Yang, B. Li, A. Zeira, Unites States Patent No.: 7, 042, 967, May 9, 2006.

[20] K. Hueske, J. Gotze, and C. V. Sinn, Optimized Channel Coding Schemes for a Guard Period Free Transmission System, in Proc. of IEEE International Conference on Acoustics, Speech and Signal Processing, pp. 2977-2980, Mar. 2008.

[21] K. Hueske and J. Gotze, Ov-OFDM: A Reduced PAPR and Cyclic Prefix Free Multicarrier Transmission System, in Proc. of 6th International Symposium on Wireless Communication Systems, pp. 206-210, Sep. 2009.

[22] D. Mattera and M.Tanda, "Preamble-based synchronization for OFDM/OQAM systems," 19th European Signal Processing Conference, Sept. 2011.

[23] C. Lele, R. Legouable and P. Siohan "Channel estimation with scattered pilots in OFDM/OQAM", Proc. SPAWC 2008, 2008.

[24] 3GPP TS36.211, "Physical Channels and Modulation", V10.4.0

[25] ITU-R Recommendation M.1225, "Guidelines for evaluation of radio transmission technologies for IMT-2000," 1997.